Comparative Analysis of Quercetin Oxidation by Electrochemical, Enzymatic, Autoxidation, and Free Radical Generation Techniques: A Mechanistic Study

AILING ZHOU AND OMOWUNMI A. SADIK*

Department of Chemistry, State University of New York—Binghamton, P.O. Box 6000, Binghamton, New York 13902

Quercetin, the most abundant flavonoid in dietary fruits and vegetables, acts as antioxidant or prooxidant depending on the environmental conditions. The antioxidant behavior is believed to involve initial oxidative steps with subsequent changes in the flavonoid skeleton, which ultimately alters the chemical and biological properties of these molecules. Although the mechanism is still unclear, it has been suggested to be strongly influenced by the surrounding media. This paper reports the oxidation of quercetin by air oxygen or autoxidation, bulk electrolysis, mushroom tyrosinase, and azodiisobutyronitrile (AIBN). The central aim of this study is to systematically examine how the similarities and differences of quercetin transformation can be affected by the nature of the oxidation systems. Using a range of molecular and structural characterization techniques (UV−vis, LC-MS, GC-MS, and NMR), the oxidation of quercetin was found to result in the generation of somewhat similar metabolites including depside, phenolic acids, and quercetin−solvent adducts, although the transformation process and quantities of each product depend on the type of oxidation method employed. The rate of quercetin autoxidation can be fitted to a monoexponential first-order decay with a k value of 6.45×10^{-2} M^{-1} s^{-1}. Comparison of quercetin oxidative products in the different systems provides a deeper insight into the underlying mechanism involved in the oxidation process. This work demonstrates that the presence of water and/or nucleophiles as well as different catalysts (tyrosinase, AIBN, or air oxygen in solution) may have very important implications for the formation of quinone with subsequent oxidative cleavage or polymerization. Moreover, the apparent first-order kinetics of autoxidation can indicate a rate-determining, one-electron oxidation of quercetin anions followed by two fast steps of radical disproportionation and solvent addition on the resulting quinone.

KEYWORDS: Quercetin; oxidation; mechanism; electrochemical; radical generator; enzyme; autoxidation; quinones

INTRODUCTION

Quercetin is a flavonol that is ubiquitous in edible plant materials and has been a subject of detailed examination for its antioxidant and other biological properties (*1, 2*). Various groups of polyphenolic compounds, such as catechins, flavonols, and anthocyanins, have been found to contribute to the nonenzymatic and enzymatic browning of foods (*3*), although the mechanism is unclear. There is increasing controversy about the beneficial effects of polyphenols in general, with questions about their benefits as antioxidants versus risks as prooxidants (*4*). From a dietary supplement/herbal medicine point of view, it is especially important to understand their behavior with respect to oxidation, because their use is being promoted on the basis of their antioxidant properties. In most cases, their antioxidant behavior involves initial oxidative steps with subsequent changes in the

flavonoid skeleton, simultaneously altering the chemical and biological properties of these molecules. In this framework, knowledge of the oxidative products under different conditions is relevant to get insight into the action of quercetin as antioxidant and/or prooxidant. Recent studies have suggested that to fully assess the health benefits of dietary polyphenols, the biological properties of both the ingested parent compound and its microbial metabolites must be investigated (*5−7*). Therefore, the study of flavonol oxidation, as well as the nature of the oxidation products and their properties, should be addressed as an issue of high significance.

Oxidation of flavon-3-ols has been studied under several oxidizing conditions, including enzymatic (*8−11*), electrochemical (*12−15*), chemical (*3*), microbial (*16−18*), and/or air oxidation (*19*), two-electron copper ion mediated oxidation (*20, 21*), superoxide anion radical (*22*), and radical generator DPPH/CAN/ AIBN treatments (*23, 24*). Such oxidation could also be promoted by the components of the tissue culture medium and/

* Corresponding author [fax (607) 777-4478; e-mail osadik@binghamton.edu.

or of the cells (enzymes, cofactors, DNA). Specifically, oxidative enzymes that occur in plant tissues such as peroxidase (POD) have been shown to act on quercetin, and more than 20 compounds could be detected by analytical HPLC and 8 oxidation products have been characterized by spectroscopic techniques (UV−vis, IR, NMR, and MS) including benzoic acid, phloroglucinol carboxylic acid, quercetinchinone, quercetin−water adduct, and polymerization products (*9*). Quercetin was oxidized with potassium ferricyanide under alkaline conditions and shown to generate the same set of products derived from its oxidation by mushroom polyphenol oxidase (PPO) and horseradish peroxidase (POD) (*3*). Some of these substances were also produced through Cu^{2+}-catalyzed oxidation and radical generator. Electrochemically, we have reported 18 oxidative products following the bulk electrolysis of quercetin under physiological environment as described in **Table 1** (*25*).

Evidently, the final oxidation products and the stability of the intermediate species resulting from the oxidative reactions are substantially different depending on the surroundings as well as the nature of oxidative process. However, there has not been any systematic study comparing the nature of the oxidation products, and it is also not clear whether one mode of oxidative transformation is preferred on the basis of the different conditions. This work provides comparative oxidative studies of quercetin using electrochemical, enzymatic, AIBN free radical generation, and autoxidation in combination with modern spectroscopic techniques, such as UV−vis spectroscopy, electrochemical techniques, HPLC with photodiode array detection, and GC-MS and LC-MS techniques. From the examinations carried out, it became clear that regardless of the mode of oxidation, quercetin oxidation appears to yield, more or less, the same set of quinone intermediates. Additional products may derive from subsequent cleavage or addition reactions of intermediate species depending on the conditions. This study provides a deeper insight into the underlying mechanism involved in the oxidation process of flavonols.

MATERIALS AND METHODS

Materials. Quercetin, tyrosinase from mushroom (EC 1.14.18.1, ≥1000 units/mg), and derivatization reagent *N,O*-bis(trimethylsilyl)trifluoroacetamide (BSTFA) + trimethylchlorosi&G 270 software. Ag/AgCl served as reference electrode for aqueous solutions, and glassy carbon was used as working electrode for CV and DPV, respectively (Bioanalytical Systems Inc.). Reticulated vitreous carbon (RVC) (BASi, West Lafayette, IN) served as working electrode for bulk electrolysis. Bulk electrolysis was used to induce an electrochemical oxidation of quercetin following the same experimental procedure as described in our previous work (*25*). Typically, about 1.5 mL of quercetin solution was collected directly from the bulk electrolysis cell at different times, and their cyclic and differential pulse voltammetry were run immediately. The CV experiments were carried out between −500 and 1500 mV versus Ag/AgCl reference electrode. All CV and DPV measurements were conducted in oxygen-free solutions that were purged with nitrogen prior to analysis. All of the experiments were carried out with 0.5 mmol L^{-1} quercetin using ethanol/PBS buffer mixture (1:1, v/v) as solvent. During the CV and DPV experiments, 50 µL of the experimental solution was sampled every 1 h and diluted with 1 mL of blank solution, and their UV−vis spectra were recorded.

Tyrosinase-Catalyzed Oxidation of Quercetin. Enzyme-catalyzed oxidation of quercetin was achieved using tyrosinase enzyme following a literature procedure with slight modification (*3, 8*). Briefly, 0.05 mL of a DMSO solution of flavonoid (2 mM) was mixed with 0.3 mL of 0.05 M sodium phosphate buffer (pH 6.82) and 1.1 mL of water. Then, 0.05 mL of the 0.05 M sodium phosphate buffer solution (pH 6.82) of tyrosinase (2500 U/mL) was added. The reaction was monitored over 3 h to record the progressive shift in the absorbance maximum. Simultaneously, 0.1 mL was withdrawn from the reaction medium every

30 min. The reaction was finally stopped by the addition of 0.02 mL of trifluoroacetic acid (30% in acetonitrile). The analysis of tyrosinase-induced oxidation products of quercetin was subsequently performed using HPLC with PDA detection.

Radical Generator AIBN Induced Oxidation of Quercetin. Free radical oxidation of quercetin was carried out using AIBN free radical generator according to prior literature procedure (*23*). A typical experiment was carried out by adding AIBN (984 mg, 6.0 mmol, 20 equiv) to a solution of quercetin (100 mg, 0.3 mmol) in CH_3CN (250 mL) with 100 µL of concentrated HCl. The temperature of the reaction mixture was maintained at 60 °C, and the reaction was completed within 40 min by real-time UV−vis analysis. Acetonitrile was then removed under reduced pressure, and the resulting solid was washed with hexane to remove the unreacted AIBN.

UV−Vis Spectroscopic Studies. UV−vis measurements were carried out using a UV−vis Hewlett-Packard diode array spectrophotometer (model HP-8553, Foster City, CA). This instrument was used to monitor the absorbance changes during autoxidation and bulk electrolysis of quercetin as well as for the radical generator mediated oxidation and tyrosinase-catalyzed oxidation of quercetin. Scans were performed over a wavelength range of 200−800 nm.

Analytical HPLC Analysis. HPLC analysis was performed on a Dionex Ultimate 3000 equipped with a photodiode array detector, Chromeleon software, and C_{18} column (250 × 4.6 mm i.d., 5 µM, Zorbax-Rx-C18, Rockland Technologies, Newport, DE). The mobile phase composition for HPLC analysis was water with 0.1% trifluoroacetic acid (CF_3COOH) (A) and 90% methanol with 0.1% CF_3COOH (B) unless otherwise noted. The gradient program started with 50% B and was maintained at 50% for 5 min, then increased linearly to 90% methanol within 30 min, kept at 90% for another 10 min, then returned to the starting conditions within 5 min with a flow rate of 0.5 mL/min unless otherwise noted. Injection was made by a Rheodyne injection valve with 20 µL fixed loop. Spectral analysis was set to scan from 210 to 600 nm.

GC-MS and LC-MS Analyses. To achieve this step, the oxidation reaction of quercetin induced by air oxygen, electrochemical, and radical generator was run ca. 10 times, respectively, and the pooled products were passed through a silica gel column (60−200, Merck). By first eluting with hexane and ethyl acetate with increasing concentrations of methanol, samples with common TLC fractions were pooled and subsequently run through a Sephadex LH-20 column (GE Healthcare, Piscataway, NJ) while eluting with methanol. Fractions with the same UV−vis profile were pooled together for GC-MS and LC-MS analysis to verify the structural nature of the oxidized products.
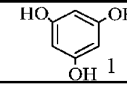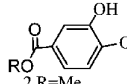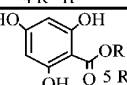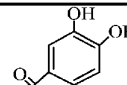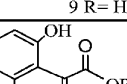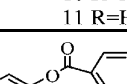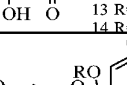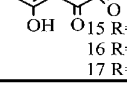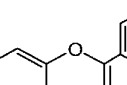
GC-MS analyses were performed on a Hewlett-Packard (HP) model GC 5890 series II gas chromatograph coupled with a HP 5973 series mass selective detector, and a HP 7683 GC autosampler was employed for all analyses. Samples were derivatized with *N,O*-bis(trimethylsilyl)trifluoroacetamide (BSTFA) + 1% trimethylchlorosilane (TMCS) and separated on a 30 m × 0.35 mm × 0.25 µm HP5MS fused silica capillary column (Agilent Technologies, Santa Clara, CA). *LC-MS* analyses were performed on a Thermo Scientific Surveyor system coupled with a PDA detector and LCQ Fleet mass spectrometer in sequence. A Thermo Hypersil GOLD C_{18} column, 100 × 2.1, 3 µM (Thermo-Fisher Scientific) was used, and the mobile phase composition for LC-MS analysis was H_2O with 10 mM ammonium formate (A) and 90% aqueous methanol with 10 mM ammonium formate (B); the gradient program was 20% B holdi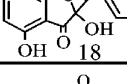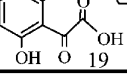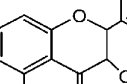ng for 1 min, ramp to 100% B over 9 min, and hold for 10 min at a flow rate of 200 µL/min. The mass spectrometer via an ESI was operated either in a negative or in a positive mode or both depending on the nature of the compound. MS/MS or MS^3 was performed as needed.

NMR Analysis. A Bruker Am 360 spectrometer operated by Tecmag NTNMR software was used for ^{1}H NMR analysis with DMSO-d_6 as solvent.

RESULTS AND DISCUSSION

UV−Vis Spectrometric Characterization. *Oxidation of Quercetin by Air Oxygen.* The facile oxidation of quercetin and other flavonols by air oxygen has been the subject of numerous

Table 1. Identified Oxidative Products of Quercetin Induced by Four Kinds of Oxidation Model[a]

Compound	Structure	Electrochemcal	Enzymatic	AIBN	Autooxidation
1	(1)	++	-	+	++
2	2 R=Me	+	-	+	+
3	3 R=Et	+	-	+	+
4	4 R=H	++	++	++	++
5	5 R=Me	+	-	+	+
6	6 R=Et	+	-	-	+
7	7 R=H	++	++	++	++
8	8 R=Me	-	-	+	-
9	9 R=H	+	-	-	-
10	10 R=Me	-	-	+	-
11	11 R=H	++	-	+	+
12	12 R=Me	-	-	++	-
13	13 R=Et	+	-	-	+
14	14 R=H	+	-	+	+
15	15 R=Me	-	-	+	-
16	16 R=Et	++	-	-	++
17	17 R=H	+	+	+	+
18	18	+	+	+	+
19	19	-	-	+	-
20	20	+	-	+	-
21	21	+	+	+	+
22	22	+	-	+	-

[a] +, detected; -, not detected; ++, main oxidized products.

publications to date, with the first report by Nierenstein in 1912 (*26*). The antioxidant behavior is believed to involve initial oxidative steps with subsequent changes in the flavonoid skeleton, which ultimately alter the chemical and biological properties of these molecules. Although the mechanism is still unclear, it has been suggested to be strongly influenced by the surrounding media. It is also important to understand their behavior with respect to oxidation, because their use is being
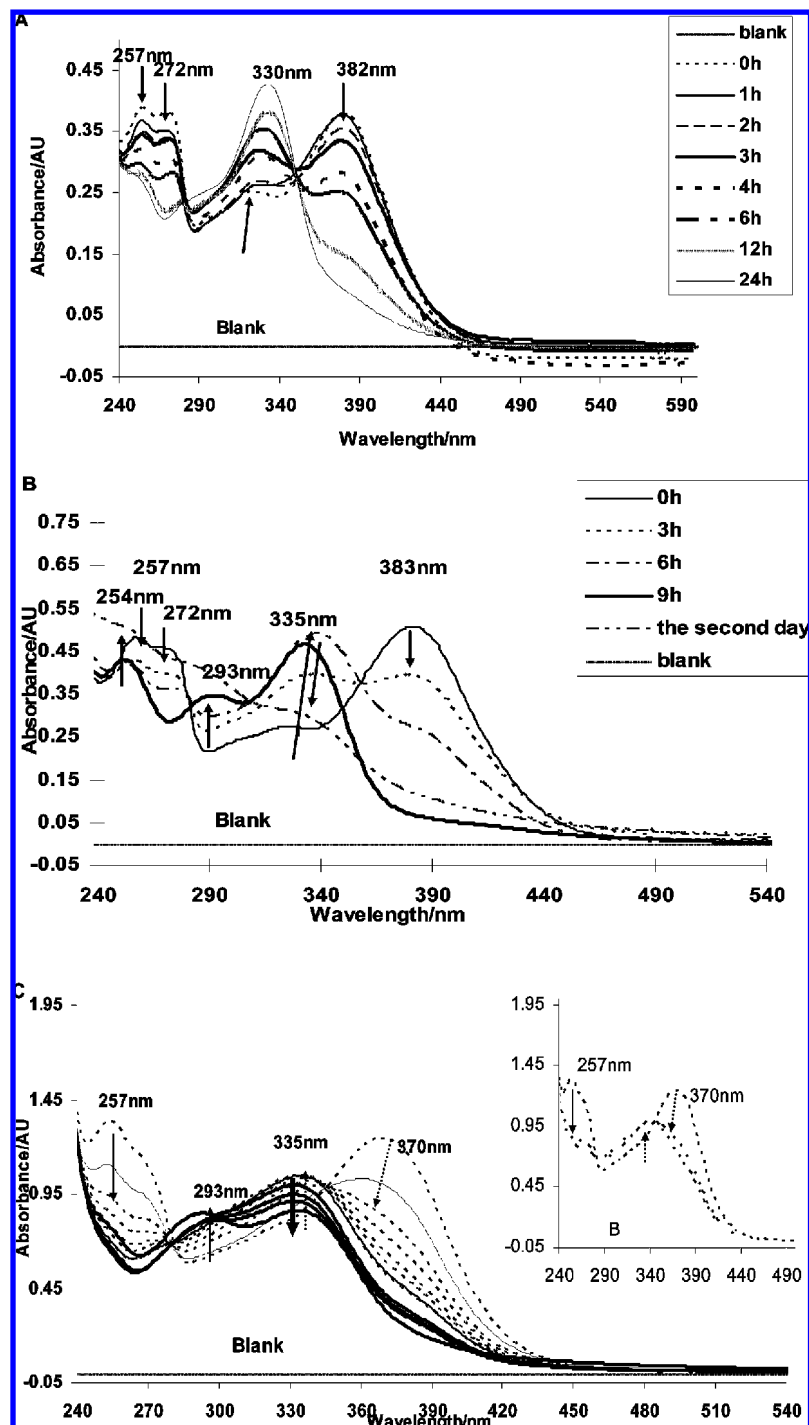
Figure 1. UV–vis spectra of quercetin oxidation (0.02 mM) through (**A**) air oxygen in ethanol/PBS buffered solution (1:1, v/v, pH7.40), (**B**) bulk electrolysis, and (**C**) mushroom tyrosinase in PBS buffer (pH 6.80). Scan speed was set at 2 min intervals for 20 min and then at 10 min intervals for a total of 3 h; the arrows designate the evolution of the peak.

promoted on the basis of their antioxidant properties. For comparison, we studied the oxidation of quercetin by air oxygen in ethanol−PBS buffered aqueous solutions under physiological pH conditions (pH 7.40). To monitor the oxidation of quercetin, 0.02 mM quercetin (prepared in cuvette) was exposed to saturated air solution. As shown in **Figure 1A**, the progressive shift of the registered spectra or instantaneous displacement of quercetin absorption maximum (380 nm) resulted in a new peak with maximum absorbance at ca. 330 nm. At the same time, the reaction was accompanied by a decrease in the absorbance at 257 nm with a shoulder at 275 nm, which was further observed to decrease in intensity with time. This was followed

by the appearance of a new peak at ca. 290 nm, and the absorbance increased at both 255 and 290 nm (data not shown), indicating that the cinnamyl system (B- and C-rings) had been completely destroyed. After 24 h of autoxidation, the concentration decreased to 4.7 μM (measured on the basis of the absorbance at λ_{380nm}), and the rate of quercetin consumption at room air O_2 concentration can be fitted to a monoexponential decay (first order with a k value of 6.45×10^{-2} M^{-1} s^{-1}). Also, there is a gradual visible color change of the solution from yellow to brown over time. However, in the case of quercetin dissolved in ethanol or methanol solution, there was no color change or significant spectral changes recorded.

Understanding the Mechanism of Quercetin Oxidation

J. Agric. Food Chem., Vol. 56, No. 24, 2008 **12085**

Electrochemical Oxidation. Electrochemical oxidation provides a gentle approach for the oxidation of quercetin and can be performed exactly at the desired potential (*13*). The results of electrochemical oxidation are relevant to interpreting the antioxidant or estrogenic behavior of quercetin and other flavonoids in vivo on the basis of their oxidation potential information (*14*). Herein, bulk electrolysis was carried out at physiological pH condition in accordance with a literature procedure in ethanol/PBS (pH 7.4) (1:1, v/v) solution (*25*). Similarly, evidence for the electrochemical oxidation of quercetin comes from the color change. To verify the formation of these intermediates during the bulk electrolysis, we collected samples at different electrolysis intervals for UV–vis spectroscopy, CV, and DPV analyses, respectively.

Interestingly, similar to the oxidation induced by air oxygen, the hypochromic shift of the characteristic absorbance at ca. 380 nm to short wavelengths of 335 nm and subsequently to 290 nm was also found during the course of bulk electrolysis (**Figure 1B**), indicating the oxidation of quercetin. Once again, such oxidation may be caused by structural changes to its functional groups including a ketone moiety, catechol on the B-ring to corresponding *o*-quinone, and phenolic moiety.

As we reported previously (*25*), the CV and DPV experiments results show that over a prolonged electrolysis time (9 h), the intensity of the first oxidation peak decreased and finally disappeared. At the same time, a more positive shift (from +0.16 V to +0.28 V) of the oxidation peak potential was observed. These could be attributed to the formation of oxidized products having higher oxidation potentials than that of the parent quercetin, suggesting a major structural change of quercetin during the bulk electrolysis.

Tyrosinase-Catalyzed Oxidation. Spectrometric study of enzyme-catalyzed quercetin oxidation can provide additional evidence for one-electron peroxidatic oxidation of quercetin and *o*-quinone formation as well as a one-electron reduction of preformed quercetin *o*-quinone (*26*). In this work, the incubation of quercetin with tyrosinase produced characteristic changes in the UV–vis spectrum, which did not occur in mixtures without enzyme or quercetin, as shown in **Figure 1C**. After the addition of tyrosinase, a new peak appeared at 335 nm and two isosbestic points were first observed at 281 and 345 nm. As the spectrophotometric experiment continued for 3 h, the changes in the UV–vis absorption spectrum started decreasing in absorbance at 335 nm but increasing at 293 nm at a slow rate. Although the formation of products with a similar absorbance characteristic (335 nm) has been reported during the electrochemical oxidation as well as that involving lactoperoxidase (LPO)- or tyrosinase-catalyzed reactions of quercetin (*27*), (*28*), this process is slightly different from that obtained using electrochemical and autoxidation approaches, in which the absorbance at 370 nm declined gradually instead of exhibiting a quick shift to 360 nm (**Figure 1C**, inset). In particular, these differences were readily observed following the isolation by HPLC with characteristic UV-absorbing products.

Radical Generator AIBN Mediated Oxidation. Radical generator AIBN mediated quercetin oxidation was also investigated. Time course studies of UV–vis analysis have shown a quick shift of the maximum absorbance to 290 nm with a shoulder at 266 nm within 40 min of reaction, and this shift was accompanied by a series of color changes from yellow to colorless to brown, confirming the oxidation of quercetin (data not shown). These oxidized products were identified on the basis of various spectral analyses in this work following the isolation by column chromatography and HPLC as discussed under LC-

MS and GC-MS Analyses, below. The chemical entity that oxidizes quercetin using the AIBN is the free radical formed following the thermal initiation reaction
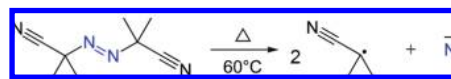

In that respect, quercetin was oxidized through a transfer of H-atoms to AIBN radicals, then the formed semiquinone radicals or quinone, which will subsequently undergo additional reactions depending on the different solvent environments (proton or nonproton solvents).

HPLC Analysis. To further characterize the complicated quercetin oxidized products, the oxidized solution was collected and monitored by HPLC with a multiple-channel PDA detector. Chromatograms are shown in **Figure 2**. **Figure 2A** shows the HPLC profiles recorded at 290 nm and spectra characteristic of the oxidized products induced by bulk electrolysis. The peak eluted at ca. 14 min in the chromatograms was identified as the parent quercetin on the basis of its characteristic spectral data. In these chromatographic profiles, it is shown that the peak intensity of quercetin decreased and new peaks gradually appeared and increased over time, indicating the oxidation of quercetin. In fact, we presented one of the chromatograms (180 min oxidation) in **Figure 3A** with a zoom in *Y* value (**Figure 3B**) to prove the complexity of the resulting oxidation products, in which at least 18 or 19 peaks were found. In particular, it is interesting to note that one of the main peaks eluted at 3.20 min with increased intensity has the UV–vis profile of 294 nm with a shoulder at 320 nm.

Compared to its UV–vis spectra obtained in ethanol–PBS (pH 7.40), the disappearance of a peak at ca. 330 nm (**Figure 1B**) may be due to the presence of acetic acid in the mobile phase composition, resulting in pH change and inherently the structural change of the oxidation products via dissociation and/or tautomerization. On the basis of its spectrometric data, a substituted benzofuranone structure (a tautomer of quercetin–water adduct, compound **17** or **18**, **Table 1**) was proposed for this peak. Hirota has reported the characteristic absorption of substituted benzofuranone, which was affected by pH, and suggested that pH-dependent changes in the absorption spectrum were due to dissociation of protons from phenolic OH groups (*29*).

In addition, it is worth noting that the peak eluted at 20 min showed UV–vis absorbance with a prominent maximum around 304 nm and a less pronounced maximum at 363 nm, suggesting the formation of quinone (compound **21**) as reported by Hvattum (*30*). The UV spectrum of compound **21** (**Figure 3C**) was analogous to that of the other three smaller peaks eluting at 21–23 min. The existence of four products with the same UV–vis profile indicates there are at least four isomeric quercetin quinones formed. It is not clear at the moment which form of the quinone (ortho-quinone or quinone methide, **Scheme 1**) is the major contributor. Furthermore, the intensity of the quinone peak did not increase much over prolonged bulk electrolysis because of the quick formation of its relative cleavage and addition products in the presence of ethanol and methanol solutions, aqueous media. In fact, due to the low solvating capacity of water and its high hydrogen-accepting properties, quercetin molecules hardly coordinate to form complex polymers in these media, and the most probable reaction pathway becomes that of oxidative degradation (*31*). As reported by Makris and Rossiter, heating of quercetin in aqueous solutions causes cleavage of its skeleton, leading to the formation of characteristic fragments, such as protocatechuic acid and phloroglucinol carboxyloic acid (*32*). We also monitored the oxidation

12086 *J. Agric. Food Chem.,* Vol. 56, No. 24, 2008

Zhou and Sadik
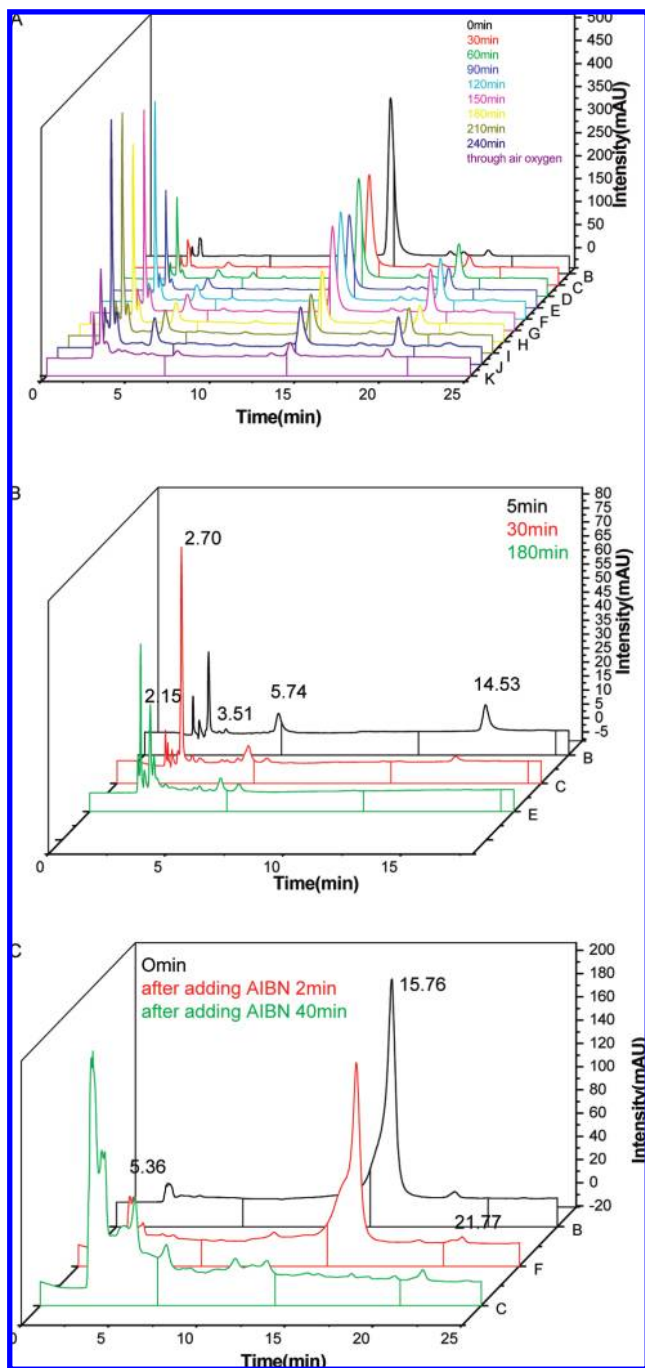
Figure 2. HPLC monitoring of the oxidation procedure of quercetin by electrochemical and autoxidation (**A**), mushroom tyrosinase (**B**), and radical generator AIBN (**C**). The mobile phase composition for the separation of tyrosinase-catalyzed oxidation products was water with 0.5% acetic acid (**A**) and 80% acetonitrile with 0.5% acetic acid (**B**). The gradient program started with 40% B, was maintained at 40% for 5 min, then was increased linearly to 80% B within 30 min and kept at 80% for another 10 min, and then was returned to the starting conditions within 5 min.

of quercetin by air oxygen under the same ethanol−PBS buffer solution. Oxidation of quercetin by air oxygen yielded a similar set of products (purple line, **Figure 2A**).

Tyrosinase is a copper protein that contains a coupled binuclear copper-active site and can show catalytic functions for a rapid, two-electron oxidation of *o*-diphenols into *o*-quinones (catecholase activity). Hitherto, the HPLC profile of the tyrosinase oxidation products of quercetin was reported by Gülşen (*11*) and Kubo (*8*), and more polar substituted benzo-
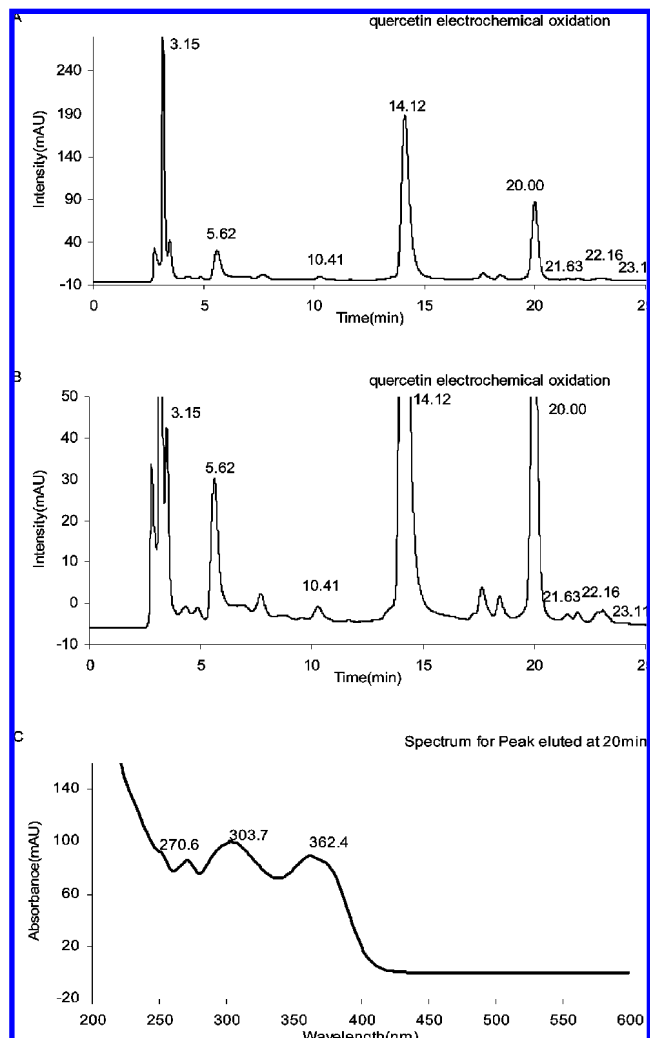
Figure 3. HPLC chromatogram of quercetin oxidation (180 min of oxidation) obtained over a prolonged bulk electrolysis (**A**) and the chromatogram with a zoom in *Y* value (**B**); peak spectrum eluted at 20.0 min (**C**).

furanone and less polar compounds (e.g., dimers) than quercetin were detected. Here, the tyrosinase-catalyzed oxidation of quercetin at pH 6.8 was carried out, and several distinctions have been found. The analysis of tyrosinase oxidation products was performed every 30 min, as shown in **Figure 2B**. By using a different chromatographic condition, the peak eluted at 5.74 min was identified as parent quercetin. The peak eluted at 14.50 min with the same UV−vis absorbance of a prominent maximum around 304 nm and less pronounced maximum at 363 nm as found in the electrochemical and air oxygen induced oxidation of quercetin, confirmed the formation of the quinone (**Figure 3C**). The quinone quickly formed and showed the maximum absorbance intensity, but it is not stable, and subsequently the peak decreased and finally disappeared. These results confirmed the change of UV−vis absorbance discussed under Tyrosinase-Catalyzed Oxidation above, where the maximum absorbance quickly switched from 370 to 360 nm instead of gradual decline of the peak at 370 nm. In addition, the peak eluted at 2.70 min with λ_{max} at 294 nm and a shoulder at 320 nm gradually increased. This spectrometric characteristic was recognized as substituted benzofuranone (compound **18**, **Table 1**) as discussed previously. This was found to be unstable, subsequently breaking down to the following two products, protocetachuic acid and phloroglucinol carboxylic acid.

Scheme 1. (**A**) Schematic of Quercetin Oxidation Induced by Bulk Electrolysis, Autoxidation, AIBN, and Tyrosinase; (**B**) Initial Oxidation Step of Quercetin Indicating the Formation of Quinone Species Intermediates
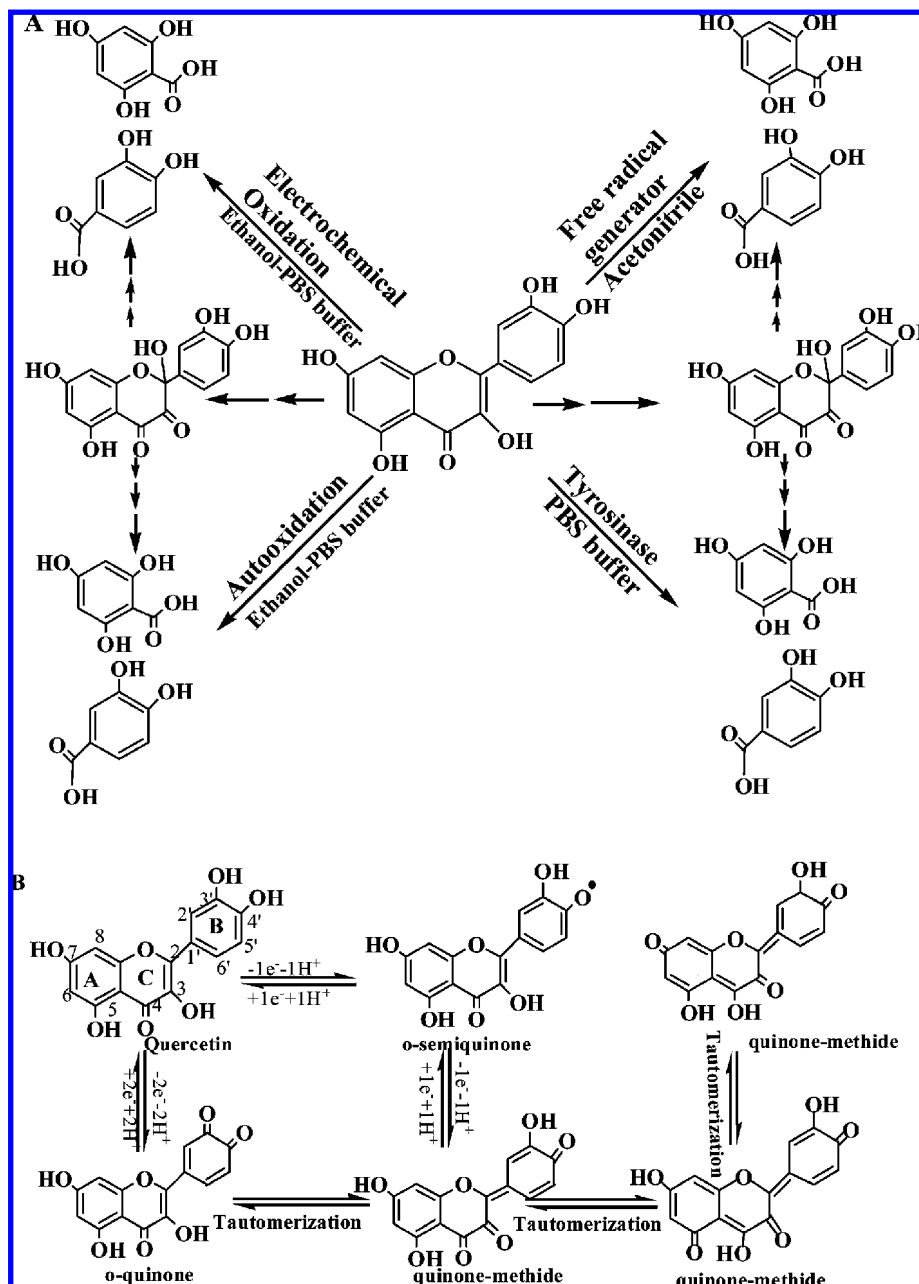
Finally, AIBN-mediated oxidation was carried out in the absence of nucleophile such as methanol or ethanol. HPLC chromatograms of AIBN radical generator mediated oxidation of quercetin over time are shown in **Figure 2C**. The oxidation process was completed within 40 min. Although we did not get good resolution of each peak in the presence of radical generator, the formation of a complex mixture was observed on the basis of the different absorbance spectrum of each peak compared to that of quercetin, indicating the oxidation of quercetin. It is also an indication the oxidation products are more polar on the basis of the different retention times. Further confirmation was carried out by using LC-MS and GC-MS techniques, respectively.

LC-MS and GC-MS Analyses. To further characterize the mixture purified by column chromatography, LC-MS and GC-MS analyses were carried out. This step excludes the characterization of tyrosinase-catalyzed oxidation products because of the microreaction. LC-MS analyses have provided characteristic

m/z values of the electrochemically oxidized products of quercetin in ethanol−PBS buffer (pH 7.40) (*25*). Here, **Table 2** shows the mass data information of the main quercetin oxidized products induced by AIBN in acetonitrile. Albeit only four products (compounds **8**, **14**, **18**, and **22**, **Table 1**) were reported by Krishnamachari (*23*), the molecular ion peak [M − -H]⁻ with *m/z* at 125, 153,169, 197, 331, 305, 333, and 319 and characteristic fragments confirmed the presence of compounds **1**, **4**, **7**, **11**, **16**, **14**, **19**, and **12**, which correspond to 2,4,6-benzenetriol, protocatechuic acid, phloroglucinol carboxylic acid, 2,4,6-trihydroxyphenylglyoxylic acid, quercetin−methanol adduct, and depside as well as the substituted depside, respectively, the latter of which is subsequently hydrolyzed to aromatic acids. These results were correlated very well with their mass data obtained using the GC-MS techniques (**Figure 4C** and **Table 3**). Compared to the electrochemical oxidation products of quercetin, the quercetin−ethanol adducts and relative ethylated esters are absent. The presence of the above mass data

12088 *J. Agric. Food Chem.,* Vol. 56, No. 24, 2008

Zhou and Sadik

Table 2. MS Data and Characteristic Fragments of Quercetin Oxidation Products Induced by AIBN from LC-MS/MS Analysis

compd	molecular ion	fragments
1	125	97, 83, 57
2	167	152,108
4	153	125, 109, 79
5	183	183, 151
7	169	151, 125, 95
8	195	167, 151, 136, 108
10	211	193, 183, 179, 151
11	197	197, 153, 125, 109
quercetin	301	301, 283, 273, 257, 179, 151
12	319	287, 275, 269, 169, 151
14	305	211, 191, 169, 151
15	331	313, 299, 287, 271, 179
compd **15** + H_2O	349	331, 299
compd **15** + CH_3OH	363	345, 331, 319, 288
17 or **18**	317	317, 299, 271, 255, 207, 191, 179, 163 151
19	333	315, 305, 301, 223, 205, 179, 151
20 (taxifolin)	303	285, 271, 259, 221, 125
21 (quinone)	299	299, 284, 271, 255, 217
unknown	343	325, 315, 301, 255, 179
22 (dimer)	601	601, 583, 557, 299

indicated that similar oxidized products were produced from the other two oxidation methods (electrochemical and free radical induced). By combining the following GC-MS data, the confirmed structural information is summarized in **Table 1**.

GC-MS analysis can be also used for the structural identification following the derivatization process using trimethylsilyl (TMS) for polar organic compounds. The GC-MS total ion chromatograms (TIC) through air oxygen, electrochemical, and radical generator induced oxidation products are shown in **Figure 4** after derivatization with BSTFA. The three TIC profiles of quercetin oxidized products through air oxygen, bulk electrolysis, and AIBN showed similarity in their oxidative products, and, obviously, bulk electrolysis of quercetin in ethanol−PBS buffer (pH 7.40) provided representative information with the higher number of peaks, as shown in **Figure 4B**. In this case, on the basis of the molecular ion (MI) and fragmentation patterns of the oxidized products, peaks eluted at 13.52, 17.48, and 21.05 min were tentatively identified as the BSTFA derivatives of compounds **1**, **4**, and **7** (2,4,6-benzenetriol, protocatechuic acid, and phloroglucinol carboxylic acid, respectively) with m/z 342, 370, and 458, respectively, and this conforms to the standard data searched in the NIST database. The MI and/or [M − CH₃] value of peaks eluted at 21.70 and 23.29 min with m/z 398 and 471 confirmed the structural assignment of 2,4-dihydroxyphenylglyoxylic acid (compound **9**) and 2,4,6-trihydroxyphenylglyoxylic acid (compound **11**). The m/z values of characterized fragments were 281 and 369, standing for the BSTFA derivatives of 2,4-dihydroxybenzoyl and the BSTFA derivatives of 2,4,6-trihydroxybenzoyl group. The MI value of peaks eluting at 31.58, 36.98, 37.54, 38.00, and 40.18 min were identified as the BSTFA derivatives of compounds **13**, **14**, and **16**, **17**, and **18** and quercetin, respectively, with m/z 622, 666, 634, 679, and 662. The above MS data were attributed to the cleavage and addition reactions of quercetin. In addition, the peaks eluted at 15.13 and 18.81 min were the trace TMS derivatives of methyl esters of both protocatechuate and 2,4,6-trihydroxybenzoate (compounds **2** and **5**), indicating that GC-MS with EI mode provided better sensitivity and higher selectivity than LC-MS. In the case of AIBN-mediated oxidation of quercetin, the peak intensity eluted at 37.99 min (compound **14**, depside) is higher than that in panels **A** and **B** of **Figure 4**. Also, BSTFA derivatives of the

methyl ester of 2,4,6-trihydroxyphenylglyoxylic acid with MI 428 (compound **10**) was found. Although the peaks eluting between 24 and 30 min in the GC-MS spectrum remained unidentified, the relative quantities of each identified component were estimated on the basis of the peak area, as shown in **Tables 1** and **3**. The first five main products were compounds **4**, **7**, **10**, **11**, and **14** with relative area percents of 24.65, 33.98, 14.45, and 5.38, respectively. Also, the quantities of the main products resulting from electrochemical oxidation and autoxidation were estimated in a similar way, with compounds **1**, **4**, and **7** having relative area percents of 12.02, 37.59, and 21.51, respectively. In the case of tyrosinase-catalyzed oxidation, the main polar products were estimated on the basis of the area in HPLC chromatograms. The quantities of the peaks eluting at 2.62 and 5.25 min were 66.10 and 14.27%, respectively, after 30 min of reaction.

¹H NMR Analysis. ¹H NMR analysis of quercetin and the main collected fractions was carried out after purification by column chromatography. All NMR experiments were run for 120 min to acquire good spectral scan integration. ¹H NMR was used to provide information on the changes in quercetin proton environment before and after oxidation. The changes can provide insight into the structural changes of quercetin and the intermediates. The oxidation of quercetin was confirmed by the disappearance of the characteristic NMR hydroxyl protons peak of parent quercetin. For example, the expected singlet peak associated with the noncoupling 5-OH proton at δ 12 of quercetin and chemical shift (δ) of the hydrogens located in the B ring in a lower field (δ 6−8 ppm) [quercetin: ¹H NMR (300M, DMSO-d_6), δ 12.50 (1H, 5-OH), 10.81 (1H,7-OH), 9.60 (1H, 3-OH), 9.39 (b, 2H, 3′,4′-OH), 7.68 (1H, H-2′), 7.54 (d,1H, H-6′), 6.88 (1H, H-8), 6.41 (1H, H-5′), 6.19 (1H, H-6) were confirmed. Moreover, we characterized three polar fractions as follows: fraction 1, ¹H NMR (300M, DMSO-d_6), δ 7.41−7.36, 6.93, 9.40; fraction 2, ¹H NMR (300M, DMSO-d_6), δ 7.32−7.42, 6.80, 9.22; fraction 3, ¹H NMR (300M, DMSO-d_6), δ14.52, 10.28, 7.26−7.32, 6.77, 5.77−5.92, 5.77, 5.62, 5.41. Compared to the quercetin, the chemical shift at δ 14.52 may contribute to the intramolecular hydrogen bonding between COOH and C═O. Also, the δ value of the hydrogen in the fractions has shifted to the high field (δ 5.92−5.41), indicating that the parent structure of quercetin has been destroyed. Current work is still focusing on structural elucidation of each quercetin oxidized product by NMR technique.

Therefore, results from the different spectroscopic techniques (UV−vis, HPLC, LC-MS, GC-MS, and NMR analyses) indicated that each mode of oxidation produced a more or less similar set of oxidized products, as shown in **Scheme 1A**. However, the mechanism of oxidation is thought to vary with the nature of the oxidizing agent, especially the preferential formation of quinone radicals and/or quinone intermediates in the initial oxidation step with different oxidation systems (**Scheme 1B**). Electrochemically, it has been reported to proceed with two steps in hydroalcoholic solution involving electrochemical step and chemical steps (*12, 25*). In that case, quercetin undergoes both one-electron oxidation and a second one-electron oxidation corresponding to the formation of quinone radical, semiquinone, o-quinone, or tautomers (p-quinone methide). In the chemical step, but for the quercetin−ethanol adduct, the water adduct species of quercetin are very unstable. These continue to undergo homogeneous chemical reactions such as intramolecular rearrangements, finally leading to the formation of a very complex mixture of polar reaction products. The variation is attributed to the fact that the oxidation of quercetin
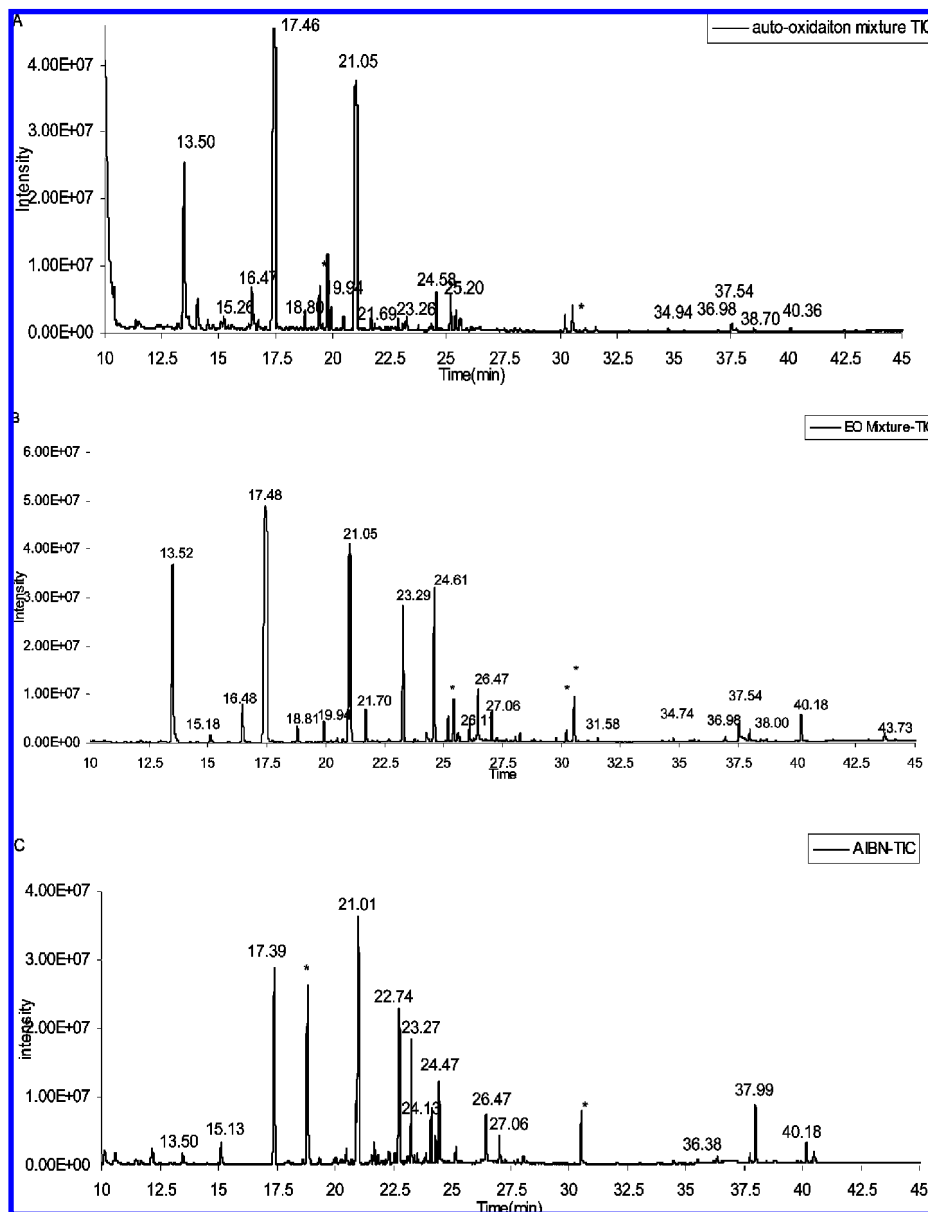
Figure 4. Total ion chromatogram (TIC) of quercetin oxidized products obtained by (**A**) air oxygen, (**B**) electrochemistry oxidation, and (**C**) radical generator AIBN by GC-MS (∗ represents peaks from column).

Table 3. Retention Times and Important Characteristic Ions, as well as Relative Area of Each Peak Present in the Mass Spectra of Quercetin Oxidation Induced by AIBN from GC-MS Analysis

| compd	time (min)	GC -MS	fragment	rel area %
1	13.50	342	342, 327, 268, 253, 147, 133	1.82
2	15.13	312	312, 281, 193, 165	2.92
4	17.39	370	370, 355, 371, 311, 281, 267, 223, 193, 137	24.65
5	18.62	400	400, 385, 369, 366	0.70
7	21.01	458	458, 443, 369, 355, 283, 207, 147	33.98
10	22.74	428	428, 369, 147	14.45
11	23.27	486	486, 471, 369, 353, 147	10.31
unknown	27.06	598	598, 583, 481, 509, 369, 147	2.58
unknown[a]	33.85	695	695, 650, 635, 608, 533, 369, 355, 281	0.39
unknown[a]	33.96	650	650, 634, 607, 577, 533, 369, 581	0.69
14	37.99	666	666, 651, 355, 281, 193, 147	5.38
17 or **18**[a]	39.35	679	679, 577, 369, 281, 147	
quercetin	40.18	662	662, 647, 575, 559, 487, 281, 207, 147	2.13
total				100

[a] Peaks from the concentrated fractions.

is not a single reaction, and subsequent side reactions lead to the formation of a series of complicated oxidized products.

Different mechanisms of quercetin transformations occur during its oxidation by air oxygen in moderately basic water

12090 *J. Agric. Food Chem.,* Vol. 56, No. 24, 2008

Zhou and Sadik

and water−ethanol solutions at ambient temperature (*19*). In this work, the apparent first-order kinetics of autoxidation can indicate a rate-determining, one-electron oxidation of quercetin anions followed by two fast steps of radical disproportionation and solvent addition on the resulting quinones (*15*). However, in the case of tyrosinase-catalyzed oxidation, the direct conversion of an *o*-diphenol to the corresponding *o*-quinone (diphenolase activity) in the presence of oxygen was preferred on the basis of the quick formation of quantities of quinone. Typically, the characterized compound, 2-(3,4-dihydroxybenzoyl)-2,4,6-trihydroxy-3(2*H*)-benzofuranone (compound **18**, **Table 1**) was found in all four of the above oxidation systems. This is believed to be formed through the complete hydration of the flavylium ion resulting from quinone, where a ring−chain tautomeric equilibrium results in the chalcan-trione (*13, 23*).

In addition, oxidation polymerization is another possible degradation pathway of quercetin, although the dimer was found in trace amounts in the current system. Interestingly, there are different versions for the structural elucidation of the formation of quercetin dimer according to the NMR data in different oxidation systems. For example, it is reported that quercetin oxidation by radical generator AIBN and potassium ferricyanide as well as cytochrome *c* was shown to form the heterodimer through a concerted reaction with the B-ring *o*-quinone moiety (*10*).
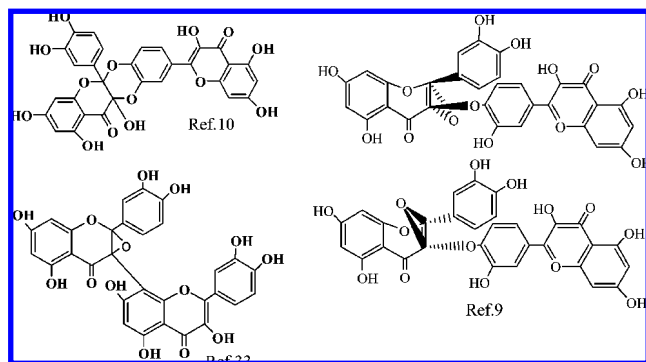
Schreier and Ramos reported two different quercetin dimer structures, respectively, and the presence of an epoxide ring between C2 and C3 was proposed (*9, 33*). However, for all of the above different structures of dimers, the same MS data with molecular ion *m/z* 601 were given in negative LC-MS analysis (*34*). The mechanism of flavonoid dimer formation has been studied by Krishnamachari (*35*), using AIBN in combination with a series of hydroxylated flavonols. The formation of flavonoid dimers was proposed to occur via radical or Diels−Alder type cycloaddition with *o*-quinone as the intermediate and the C2−C3 olefinic system in the second unit. It is also believed to occur by the presence of a free C-3 hydroxyl, coupled with a B-ring ortho hydroxyl unit, and the B-ring with *o*-diphenol feature seems to play a central role in the whole oxidation process. Nevertheless, the hypothesis of dimer formation should be carefully considered because it is based upon the observation of radical reactions in organic media; the formation of quinone in the buffered aqueous solutions during dismutation could not be excluded.

The quantitative differences in the level of quinone observed in the chromatograms from the above four oxidation methods suggest that the formation of quercetin dimer may be dependent on the formation of quercetin radicals, quinone, or semiquinone intermediates. Therefore, the presence of water and/or nucleophiles as well as different catalysts tyrosinase, AIBN, or air oxygen in solution may have very important implications for the formation of quinone and further oxidative cleavage or oxidative polymerization.

In summary, we have compared the oxidation of quercetin by air oxygen, electrochemical techniques, enzyme-catalyzed, and free radical generator AIBN. The findings so far have shown that, in each case, the oxidation of quercetin may yield, more or less, the same set of oxidized products. However, the real-time monitoring assay of each oxidation reaction by UV−vis and HPLC analysis demonstrates that the oxidation mechanisms are different depending on the quantity and order of appearance of each oxidized products. The results obtained here confirmed as well as supplement earlier findings regarding the oxidation of quercetin. It is expected that this study of the oxidative degradation of quercetin under different conditions will greatly facilitate the interpretation of wider epidemiological data relevant to processed fruits and vegetables, interaction with microbiota, etc. It may thus provide greater insight into understanding their complex biological activity.

LITERATURE CITED

(1) Zern, T. L.; Wood, R. J.; Greene, C.; West, K. L.; Liu, Y. Z.; Aggarwal, D.; Shachter, N. S.; Fernandez, M. L. Grape polyphenols exert a cardioprotective effect in pre- and postmenopausal women by lowering plasma lipids and reducing oxidative stress. *J. Nutr.* **2005**, *135* (8), 1911–1917.

(2) Lee, K. W.; Lee, H. J. The roles of polyphenols in cancer chemoprevention. *Biofactors* **2006**, *26* (2), 105–121.

(3) Makris, D. P.; Rossiter, J. T. An investigation on structural aspects influencing product formation in enzymic and chemical oxidation of quercetin and related flavonols. *Food Chem.* **2002**, *77* (2), 177–185.

(4) Lambert, J. D.; Sang, S. M.; Yang, C. S. Possible controversy over dietary polyphenols: benefits vs risks. *Chem. Res. Toxicol.* **2007**, *20* (4), 583–585.

(5) Rechner, A. R.; Smith, M. A.; Kuhnle, G.; Gibson, G. R.; Debnam, E. S.; Srai, S. K. S.; Moore, K. P.; Rice-Evans, C. A. Colonic metabolism of dietary polyphenols: influence of structure on microbial fermentation products. *Free Radical Biol. Med.* **2004**, *36* (2), 212–225.

(6) Rechner, A. R.; Kuhnle, G.; Bremner, P.; Hubbard, G. P.; Moore, K. P.; Rice-Evans, C. A. The metabolic fate of dietary polyphenols in humans. *Free Radical Biol. Med.* **2002**, *33* (2), 220–235.

(7) Konishi, Y. Transepithelial transport of microbial metabolites of quercetin in intestinal Caco-2 cell monolayers. *J. Agric. Food Chem.* **2005**, *53*, 601–607.

(8) Kubo, I.; Nihei, K.; Shimizu, K. Oxidation products of quercetin catalyzed by mushroom tyrosinase. *Bioorg. Med. Chem.* **2004**, *12* (20), 5343–5347.

(9) Schreier, P.; Miller, E. Studies on flavonol degradation by peroxidase(donor:H₂O₂-oxidoreductase, EC 1.11.1.7: Part 2−quercetin. *Food Chem.* **1984**, *18*, 301–307.

(10) Awad, H. M.; Boersma, M. G.; Vervoort, J.; Rietjens, I. Peroxidase-catalyzed formation of quercetin quinone methide-glutathione adducts. *Arch. Biochem. Biophys.* **2000**, *378* (2), 224–233.

(11) Gulsen, A.; Makris, D. P.; Kefalas, P. Biomimetic oxidation of quercetin: Isolation of a naturally occurring quercetin heterodimer and evaluation of its in vitro antioxidant properties. *Food Res. Int.* **2007**, *40* (1), 7–14.

(12) Timbola, A. K.; de Souza, C. D.; Giacomelli, C.; Spinelli, A. Electrochemical oxidation of quercetin in hydro-alcoholic solution. *J. Braz. Chem. Soc.* **2006**, *17* (1), 139–148.

(13) Jorgensen, L. V.; Cornett, C.; Justesen, U.; Skibsted, L. H.; Dragsted, L. O. Two-electron electrochemical oxidation of quercetin and kaempferol changes only the flavonoid C-ring. *Free Radical Res.* **1998**, *29* (4), 339–350.

(14) Yang, B.; Arai, K.; Kusu, F. Electrochemical behaviors of quercetin and kaempferol in neutral buffer solution. *Anal. Sci.* **2001**, *19*, 987–989.

Understanding the Mechanism of Quercetin Oxidation

J. Agric. Food Chem., Vol. 56, No. 24, 2008 **12091**

(15) Jovanovic, S. V.; Steenken, S.; Iara, Y. I.; Simic, M. G. Reduction potentials of flavonoid and model phenoxyl radicals. Which ring in flavonoids is responsible for antioxidant activity? *J. Chem. Soc., Perkin Trans. 2* **1996**, 2497–2504.

(16) Braune, A.; Gàùtschow, M.; Engst, W.; Blaut, M. Degradation of quercetin and luteolin by *Eubacterium ramulus. Appl. Environ. Microbiol.* **2001**, *67* (12), 5558–5567.

(17) Schneider, H.; Blaut, M. Anaerobic degradation of flavonoids by *Eubacterium ramulus. Arch. Microbiol.* **2000**, *173* (1), 71–75.

(18) Schneider, H.; Schwiertz, A.; Collins, M. D.; Blaut, M. Anaerobic transformation of quercetin-3-glucoside by bacteria from the human intestinal tract. *Arch. Microbiol.* **1999**, *171* (2), 81–91.

(19) Zenkevich, I. G.; Eshchenko, A. Y.; Makarova, S. V.; Vitenberg, A. G.; Dobryakov, Y. G.; Utsal, V. A. Identification of the products of oxidation of quercetin by air oxygen at ambient temperature. *Molecules* **2007**, *12* (3), 654–672.

(20) Jungbluth, G.; Rühling, I.; Ternes, W. Oxidation of flavonols with Cu(II), Fe(II) and Fe(III) in aqueous media. *J. Chem. Soc., Perkin Trans. 2* **2000**, 1946–1952.

(21) Utaka, M.; Takeda, A. Copper(II)-catalyzed oxidation of quercetin and 3-hydroxyflavone. *J. Chem. Soc., Chem. Commun.* **1985**, (24), 1824–1826.

(22) Kano, K.; Mabuchi, T.; Uno, B.; Esaka, Y.; Tanaka, T.; Iinuma, M. Superoxide anion radical-induced dioxygenolysis of quercetin as a mimic of quercetinase. *J. Chem. Soc., Chem. Commun.* **1994**, 593–594.

(23) Krishnamachari, V.; Levine, L. H.; Pare, P. W. Flavonoid oxidation by the radical generator AIBN: A unified mechanism for quercetin radical scavenging. *J. Agric. Food Chem.* **2002**, *50*, 4357–4363.

(24) Dangles, O.; Fargeix, G.; Dufour, C. One-electron oxidation of quercetin and quercetin derivatives in protic and non protic media. *J.Chem. Soc., Perkin Trans. 2* **1999**, (7), 1387–1395.

(25) Zhou, A. L.; Kikandi, S.; Sadik, O. A. Electrochemical degradation of quercetin: Isolation and structural elucidation of the degradation products. *Electrochem. Commun.* **2007**, *9* (9), 2246–2255.

(26) Nierenstein, M.; Whedale, M. Anthocyanin. I. Anthocyanin-like oxidation products of quercetin. *Ber. Dtsch. Chem. Ges.* **1912**, 3487–3491.

(27) Metodiewa, D.; Jaisvale, A. K.; Cenas, N.; Dickaneaité, E.; Segura Aguilar, J. Quercetin may act as a cytotoxic prooxidant after its metabolic activation to semiquinone and quinoidal product. *Free Radical Biol. Med.* **1999**, *26*, 107–116.

(28) Kubo, I.; Nitoda, T.; Nihei, K. I. Effects of quercetin on mushroom tyrosinase and B16-F10 melanoma cells. *Molecules* **2007**, *12* (5), 1045–1056.

(29) Hirota, S.; Takahama, U.; Ly, T. N.; Yamauchi, R. Quercetin-dependent inhibition of nitration induced by peroxidase/H_2O_2/ nitrite systems in human saliva and characterization of an oxidation product of quercetin formed during the inhibition. *J. Agric. Food Chem.* **2005**, *53*, 3265–3272.

(30) Hvattum, E.; Stenstrø´m, Y.; Ekeberg, D. Study of the reaction products of flavonols with 2,2-diphenyl-1-picrylhydrazyl using liquid chromatography coupled with negative electrospray ionization tandem mass spectrometry. *J. Mass Spectrom.* **2004**, *39*, 1570–1581.

(31) Pinelo, M.; Manzocco, L.; Nuñez, M. J.; Nicoli, M. C. Solvent effect on quercetin antioxidant capacity. *Food Chem.* **2004**, *88*, 201–207.

(32) Makris, D. P.; Rossiter, J. T. *High-Performance Liquid Chromatography Studies on Free-Radical Oxidation of Flavovols*; Special Publication 255; Royal Society of Chemistry: London, U.K., 2001; pp 249−251.

(33) Ramos, F. A.; Takaishi, Y.; Shirotori, M.; Kawaguchi, Y.; Tsuchiya, K.; Shibata, H.; Higuti, T.; Tadokoro, T.; Takeuchi, M. Antibacterial and antioxidant activities of quercetin oxidation products from yellow onion (*Allium cepa*) skin. *J. Agric. Food Chem.* **2006**, *54*, 3551–3557.

(34) Cherviakovsky, E. M.; Bolibrukh, D. A.; Baranovsky, A. V.; Vlasova, T. M.; Kurchenko, V. P.; Gilep, A. A.; Usanov, S. A. Oxidative modification of quercetin by hemeproteins. *Biochem. Biophys. Res. Commun.* **2006**, *342* (2), 459–464.

(35) Krishnamachari, V.; Levine, L. H.; Zhou, C.; Paré, P. W. In vitro flavon-3-ol oxidation mediated by a B ring hydroxylation pattern. *Chem. Res. Toxicol.* **2004**, *17*, 795–804.